PHYSICAL REVIEW D **87,** 114018 (2013)

Proton (antiproton) elastic scattering at energies from FNAL to the LHC in the tripole Pomeron-Odderon model

E. Martynov*

Bogolyubov Institute for Theoretical Physics, 03680 Kiev, Ukraine

(Received 19 May 2013; published 20 June 2013)

The model of elastic scattering amplitudes dominated by the triple (at $t = 0$) Pomeron pole suggested earlier is modified to confront to existing experimental data on pp and $\bar{p}p$ total and differential cross sections at $\sqrt{s} \geq 19$ GeV and $|t| \leq 14.2$ GeV^2 including the newest TOTEM data. Predictions for the future TOTEM measurements at 13 and 14 TeV are given.

DOI: 10.1103/PhysRevD.87.114018 PACS numbers: 13.85.−t, 11.55.Jy, 13.85.Dz, 13.85.Lg

I. INTRODUCTION

The TOTEM experiment at LHC provides, in fact, the first measurements of soft Pomeron contribution (more exactly of Pomeron and Odderon) because the contributions of secondary or subasymptotic Reggeons are very small at such high energies. It means that the precise measurement of pp total and differential cross sections [1–3] gives a possibility to discriminate the various Pomeron models by comparing their predictions with new data. Generally speaking, the TOTEM results are going to be a strong restriction for various phenomenological Pomeron models [1]. Many of them being directly extrapolated to 7 TeV could not describe the recent TOTEM data though they are in a good agreement with data at $\sqrt{s} \leq 1.96$ TeV. Moreover, even basing on the total cross section measurement at 7 and 8 TeV only, one can conclude that σ_{tot}^{pp} rises with energy faster than $\ln s$. Therefore some of the models have to be rejected despite its excellent agreement with the data available before LHC epoch. For example, the dipole Pomeron model with trajectory intercept $\alpha(0) = 1$ (see [4] and references therein) is unable to give $\sigma_{\text{tot}}^{pp} > 94$ mb at $\sqrt{s} = 7$ TeV.

The current state of the elastic scattering model market is given in [5] and in the comprehensive review [6]. Obviously, all the models must be verified for a consistency with new data. Many of them, if not all, require some modification to be successfully extrapolated to new data.

In [7] such a procedure was performed for the eikonal [8,9] and U-matrix [10] models. It was shown that adding the second Odderon term solves the problem only partially, a further modification of the model is necessary. Eikonal and U-matrix models are treated as infinite series of multiple input Reggeon exchanges. However, another approach to constructing the model is also possible. One can just take into account unitarity and analyticity requirements from the beginning as well as experimental information on the cross sections (e.g., increase of total cross sections) to determine the form of amplitude.

Following this idea in [4] we have suggested the tripole Pomeron-Odderon model of elastic pp and $\bar{p}p$ scattering amplitudes and compared it with data. Amplitudes in the model at very high energies are dominated by Pomeron contribution which corresponds to a pair of the branch points colliding at $t = 0$ and at the angular momentum $j = 1$ to generate a triple pole. Besides the set of the preasymptotic terms, even and odd, have been incorporated in the model. The structure of leading singularities is different from those of the well-known maximal Pomeron and Odderon model [11–13]. It was shown that the model [13] is in a good agreement with the data in a wide interval of energy and momenta transferred, but now we have found that those models without changes fail to describe the recent TOTEM $d\sigma/dt$ data.

In the present paper we are focused on our parametrization of the tripole Pomeron-Odderon model [4] exploring its simplified form (neglecting the cut contributions unimportant at high energies). This model in Ref. [4] was applied at $|t| \leq 6$ GeV^2. We add two additional terms decreasing at high $|t|$ as $1/|t|^4$ in order to extend the model for larger $|t|$. Such terms allow us (as it was shown in [13]) to describe the $d\sigma/dt$ data at $|t| \gtrsim 6$ GeV^2.

We remind of the important properties of the tripole Pomeron-Odderon model, argue its modification for high $|t|$, then we present the results of the fit and give predictions for the TOTEM measurements at higher energies and $|t|$.

II. TRIPOLE POMERON MODEL

A. The leading high energy terms of the amplitude

As it was stressed in [4], the contribution to the partial amplitude of a triple pole with linear trajectory

$$\phi(j, t) = \frac{\beta(j, t)}{[j - 1 - \alpha' t]^3} \tag{1}$$

violates the unitarity inequality $\sigma_{\text{el}}(s) \leq \sigma_{\text{tot}}(s)$. The correct Pomeron singularity dominating the partial wave is the following:

$$\varphi_{1\mathcal{P}}(j, t) = \eta(j) \frac{\beta_1(j, t)}{[(j - 1)^2 - kt]^{3/2}}. \tag{2}$$

*martynov@bitp.kiev.ua

The black disk model holds the same singularity of the partial amplitude. The imaginary part of black disk amplitude in the impact parameter representation has a steplike form with the height $1/2$ and the width equal to $R^2(s) \propto \ln^2 s$. It leads to $\sigma_{\rm tot}(s) \propto \sigma_{\rm el}(s) \propto \ln^2(s/s_0)$, $s_0 = 1$ GeV^2.

It seems to be natural to keep the same structure of singularity for subleading terms changing only their multiplicity. Our choice of subleading terms is the following:

$$\varphi_{2\mathcal{P}}(j,t) = \eta(j)\frac{\beta_2(j,t)}{[(j-1)^2 - kt]}, \tag{3}$$

$$\begin{aligned}\varphi_{3\mathcal{P}}(j,t) &= \eta(j)\frac{\beta_3(j,t)}{[(j-1)^2 - kt]^{1/2}},\\ \eta(j) &= \frac{1 + e^{-i\pi j}}{-\sin \pi j}.\end{aligned} \tag{4}$$

Thus the leading Pomeron contribution to partial amplitude has a form

$$\varphi_{\mathcal{P}}(j,t) = \varphi_{1\mathcal{P}}(j,t) + \varphi_{2\mathcal{P}}(j,t) + \varphi_{3\mathcal{P}}(j,t). \tag{5}$$

Taking into account that

$$\frac{1}{(\omega^2+\omega_0^2)^{3/2}} = \frac{1}{2\omega_0}\int_0^\infty dx x e^{-x\omega} J_1(\omega_0 x), \tag{6}$$

$$\frac{1}{\omega^2+\omega_0^2} = \frac{1}{\omega_0}\int_0^\infty dx e^{-x\omega}\sin(\omega_0 x), \tag{7}$$

$$\frac{1}{(\omega^2+\omega_0^2)^{1/2}} = \int_0^\infty dx e^{-x\omega} J_0(\omega_0 x), \tag{8}$$

where $J_{0,1}(\omega_0 x)$ are the Bessel functions, one can write the main Pomeron part of amplitude in the (s,t) representation

$$\begin{aligned}\mathcal{P}(s,t) &= iz\{\mathcal{P}_1(s,t) + \mathcal{P}_2(s,t) + \mathcal{P}_3(s,t)\},\\ \mathcal{P}_1(s,t) &= g_1^{\mathcal{P}} v_1^{\mathcal{P}}(t)\xi\frac{2J_1(\xi\tau_+)}{\tau_+},\\ \mathcal{P}_2(s,t) &= g_2^{\mathcal{P}} v_2^{\mathcal{P}}(t)\frac{\sin(\xi\tau_+)}{\tau_+},\\ \mathcal{P}_3(s,t) &= g_3^{\mathcal{P}} v_3^{\mathcal{P}}(t) J_0(\xi\tau_+),\end{aligned} \tag{9}$$

where $g_i^{\mathcal{P}} v_i^{\mathcal{P}}(t)$ are the vertex functions with $v_{i\mathcal{P}}(0) = 1$, $\xi = \ln(-iz/z_0)$, z is defined below by Eq. (11), and $\tau_+ = r_+\sqrt{-t/t_0}$, $t_0 = 1$ GeV^2, $g_i^{\mathcal{P}}$, r_+, and z_0 are constants.

Strictly speaking the amplitudes in Regge models depend on s through the $\cos\theta_t$, cosine of the scattering angle in the t channel, which for pp scattering in the center mass system has the form

$$\begin{aligned}\cos\theta_t &= 1 + 2s/(t-4m_p^2)\\ &= (t + 2s - 4m_p^2)/(t-4m_p^2).\end{aligned} \tag{10}$$

In the considered kinematical region the t in the numerator of Eq. (10) can be neglected. However we keep $4m_p^2$ because for $t = 0$ we take into account the data on cross sections at low energies, $\sqrt{s} \gtrsim 5$ GeV. Absorbing factor $1/(t-4m_p^2)$ into the vertex functions we define the energy variable as the following:

$$z = 2s - 4m_p^2. \tag{11}$$

We propose to keep the same singularity structure for the leading terms of the crossing-odd part of amplitude. However, taking into account the fact that there is no visible Odderon contribution at $t = 0$ we multiply each Odderon term by factor t:

$$\begin{aligned}\mathcal{O}(s,t) &= zt\{\mathcal{O}_1(s,t) + \mathcal{O}_2(s,t) + \mathcal{O}_3(s,t)\},\\ \mathcal{O}_1(s,t) &= g_1^{\mathcal{O}} v_1^{\mathcal{O}}(t)\xi\frac{2J_1(\xi\tau_-)}{\tau_-},\\ \mathcal{O}_2(s,t) &= g_2^{\mathcal{O}} v_2^{\mathcal{O}}(t)\frac{\sin(\xi\tau_-)}{\tau_-},\\ \mathcal{O}_3(s,t) &= g_3^{\mathcal{O}} v_3^{\mathcal{O}}(t) J_0(\xi\tau_-),\end{aligned} \tag{12}$$

where $v_i^{\mathcal{O}}(0) = 1$, $\tau_- = r_-\sqrt{-t/t_0}$ and $g_i^{\mathcal{O}}$ are the constants.

We would like to emphasize that similar (but not the same) models for $\mathcal{P}$ and $\mathcal{O}$ were considered in [11–13]. These models have the same dominating even term $\mathcal{P}_1(s,t)$ but the different subasymptotic terms $\mathcal{P}_2(s,t)$ $\mathcal{P}_3(s,t)$. The Odderon terms included in those amplitudes do not vanish at $t = 0$. The properties of the models [11,12] and their defects have been discussed in detail in [4]. They were modified in [13], defects were eliminated and a good description of data at energies up to 1.8 TeV has been obtained. However, as was noticed in [14] such a maximal Odderon term [$\mathcal{O}_1(s,t)/t$ in our notations] gives rise to the contradiction with unitarity in the models where $\sigma_{\rm el}(s)/\sigma_{\rm tot}(s) \to \text{const} \le 1$ at $s \to \infty$. In spite of this fact, we refit the model [13] (without the cuts important only at low energies) at the energies $\sqrt{s} > 19$ GeV, including TOTEM data, but we fail to describe the data qualitatively.

B. The subleading Reggeons and powerlike behaved terms of amplitudes

In [4] the described model was applied to analysis of the $d\sigma/dt$ data at $\sqrt{s} > 6$ GeV, where not only contributions of the Pomeron and secondary Reggeons but also their rescatterings (or cuts) are very important. Besides, the considered momenta transfer were restricted by $|t|_{\rm max} = 6$ GeV^2. Here we would like to check a principal possibility of the model to describe an interpolation between GeV and TeV energy region. We investigate as well which amplitude terms are important for that and which form of vertex functions $gv(t)$ is more suitable for $d\sigma/dt$ at $|t| \gtrsim 5$ GeV^2. Thus, we consider high energy pp and $\bar{p}p$ elastic scattering, starting from FNAL energy 19 GeV. We do hope that in this energy interval we can neglect at least all cuts

reducing the number of adjustable parameters. These terms are important at lower energies but their parametrization should be chosen being consistent with a good description of high energy data.

We keep in amplitudes also the standard "soft" Pomeron and Odderon, simple j poles with linear trajectories $\alpha(t) = 1 + \alpha' t$:

$$P(s,t) = -g_P \upsilon_P(t)(-iz/z_1)^{1+\alpha'_P t}, \quad z_1 = 1\ \text{GeV}^2, \tag{13}$$

$$O(s,t) = itg_O \upsilon_O(t)(-iz/z_1)^{1+\alpha'_O t}. \tag{14}$$

To describe the behavior of the $\sigma_{\text{tot}}(s)$, $\rho)(s)$, $d\sigma/dt(s,t)$ at low energy and low $|t|$ the usual secondary crossing-even and odd Reggeons ($f, a_2, \omega, \rho, \ldots$ Reggeons with intercepts $\alpha(0) \approx 0.4$–0.7) have to be included in the amplitudes. However, analyzing pp and $\bar{p}p$ amplitudes only it is sufficient to consider at $\sqrt{s} > 5$ GeV one effective even Reggeon and one effective odd Reggeon:

$$R_\pm(s,t) = \begin{pmatrix} -1 \\ i \end{pmatrix} g_\pm \upsilon_\pm(t)(-iz/z_1)^{\alpha_\pm(0)+\alpha'_\pm t}. \tag{15}$$

A preliminary analysis of the data was performed to understand how a behavior of $d\sigma/dt$ (at $|t| \gtrsim 5\ \text{GeV}^2$) can be described. We found that a correct description of these data is provided by the terms behaving as $1/(-t)^4$ at large $|t|$ (which are almost independent on s). Therefore we add to the amplitudes crossing even and odd terms $\text{Ev}(s,t)$ and $\text{Od}(s,t)$ with arbitrary phases. To decrease an influence of these terms on the amplitudes at small $|t|$ we introduce the factor $(-t)$. It would be reasonable to construct them in a more customary (Regge-like) form at small t and power-like behaving at large t . But as we noticed above our aim is, first of all, to check some principal possibilities of the tripole Pomeron and Odderon models. Therefore to avoid an extra number of parameters we choose these terms in a simplified form:

$$\text{Ev}(s,t) = i(-t)z\frac{g_{r+} + ig_{i+}}{(1 - t/t_{\text{Ev}})^5}, \tag{16}$$

$$\text{Od}(s,t) = (-t)z\frac{g_{r-} + ig_{i-}}{(1 - t/t_{\text{Od}})^5}. \tag{17}$$

Thus, the pp and $\bar{p}p$ amplitudes in a general case are defined as follows:

$$A^{\bar{p}p}_{pp}(s,t) = \mathcal{P}(s,t) + P(s,t) + R_+(s,t) + \text{Ev}(s,t) \pm (\mathcal{O}(s,t) + O(s,t) + R_-(s,t) + \text{Od}(s,t)), \tag{18}$$

where $\mathcal{P}$, $\mathcal{O}$, P, O, $R_\pm$, Ev, Od are given by Eqs. (9) and (12)–(17), correspondingly.

C. Choice of the vertex functions $\upsilon(t)$

We have considered two options for the vertex functions $\upsilon(t)$ in the Pomeron [$\mathcal{P}(s,t)$, $P(s,t)$] and Odderon [$\mathcal{O}(s,t)$, $O(s,t)$] terms.

Model I.—Exponential form:

$$\begin{aligned} \upsilon^{\mathcal{P}}_i(t) &= \exp(2b^{\mathcal{P}}_i t), & \upsilon^{\mathcal{O}}_i(t) &= \exp(2b^{\mathcal{O}}_i t), \\ \upsilon_P(t) &= \exp(2b_P t), & \upsilon_O(t) &= \exp(2b_O t). \end{aligned} \tag{19}$$

Model II.—Power form:

$$\begin{aligned} \upsilon^{\mathcal{P}}_i(t) &= (1 - b^{\mathcal{P}}_i t)^{-4}, & \upsilon^{\mathcal{O}}_i(t) &= (1 - b^{\mathcal{O}}_i t)^{-5}, \\ \upsilon_P(t) &= (1 - b^P_i t)^{-4}, & \upsilon_O(t) &= (1 - b^O_i t)^{-5}. \end{aligned} \tag{20}$$

The behavior with -5 for Odderon vertices is taken because Odderon terms of amplitudes [Eqs. (12) and (14)] have been multiplied by the factor t.

In both models the vertices for secondary Reggeons $R_\pm(s,t)$ are chosen in an exponential form:

$$\upsilon_\pm(t) = \exp(2b_\pm t). \tag{21}$$

$R_\pm(s,t)$ are negligible at high $|t|$ because of large slopes of their trajectories. However, these terms of amplitude become important at small $|t|$ where exponential vertices are reasonable.

The following normalization of $p(\bar{p})p \to p(\bar{p})p$ amplitude is used:

$$\sigma_t = \frac{k}{F_0}\Im m A(s,0), \qquad \frac{d\sigma}{dt} = \frac{k}{F}|A(s,t)|^2, \tag{22}$$

where

$$F_0 = \sqrt{(s - 2m_p^2)^2 - 4m_p^4} = 2p_p^{\text{lab}}\sqrt{s}, \qquad F = 16\pi F_0^2, \quad k = 0.3893797\ \text{mb} \cdot \text{GeV}^{-2} \tag{23}$$

and p_p^{lab} is the momentum of initial proton (antiproton) in the laboratory system of another proton. The amplitudes and couplings g are dimensionless with this normalization.

III. CONFRONTING THE MODELS TO THE DATA

A. The data

The constructed models were compared with the pp and $\bar{p}p$ data on $\sigma_{\text{tot}}(s)$, $\rho(s)$ and $d\sigma(s,t)/dt$ in the following region of s and t:

$$\begin{aligned} &\text{for } \sigma_{\text{tot}}(s), \rho(s) \quad \text{at } 5\ \text{GeV} \le \sqrt{s} \le 8\ \text{TeV}, \\ &\text{for } d\sigma(s,t)/dt \quad \text{at } 19\ \text{GeV} < \sqrt{s} \le 7\ \text{TeV} \\ &\qquad \text{and} \quad 0.01\ \text{GeV}^2 \le |t| \le 14.2\ \text{GeV}^2. \end{aligned} \tag{24}$$

The cosmic ray data on the pp total cross sections were not included in the fit procedure.

The data set we used for adjusting the model parameters has been proposed in [15], where a coherent set of all

TABLE I. Number of experimental points used for the fitting.

	$\sigma_{\rm tot}$	ρ	$d\sigma/dt$
pp	107	64	1633
$\bar{p}p$	59	11	510

existing data for $4 \le \sqrt{s} \le 1800$ GeV and $0 \le |t| \le 14.2$ GeV^2 has been built. A detailed study of the systematic errors of the data from more than 260 subsets of the data from more than 80 experimental papers have performed (original data and the corresponding references can be found in the HEP DATA system [16,17]). The corrected data are collected and written in a common format. We suggest to use this data set as a *standard data set*. The latest (with some corrections) updated version of it including TOTEM [1–3] and D0 [18] data is available online [19].

The set used for the given analysis contains 2384 points in the region described above (numbers of points for measured quantities are given in the Table I). 31 points from the 3 groups, 8 points at $\sqrt{s} = 26.946$ GeV, 11 points at 30.7 GeV and 12 points at 53.018 GeV only for $d\sigma_{pp}/dt$ were excluded from all the data presented in [17] because these groups are strongly deviated from the rest data points and can slightly distort the fit.

B. Results of the fit

At the first step we have considered Models I and II without contribution of $P(s,t)$ and $O(s,t)$ in order to see how these terms are important. We found out that such simple models quite well describe the data. The values of χ^2/dof (dof $= N_{\rm exp.points} - N_{\rm parameters}$) for all the considered parametrizations are given in Table II. The different numbers of parameters in Models I and II for the case $P(s,t)$, $O(s,t) \neq 0$ are obtained because some of the parameters b are fixed at the low limit $b = 0$. The full sets of parameters and corresponding errors for these cases are presented in Table III.

As one can see from Figs. 1–5 and from Table II, all models, even the simplest one with $P(s,t) = O(s,t) = 0$, describe quite well the experimental data. The theoretical curves in the models differ in some details but nevertheless they are globally in agreement with experimental data. Moreover, one can obtain a very similar description of the data with the following vertices:

TABLE II. The values of χ^2 and number of parameters in the considered models.

	χ^2/dof ($N_{\rm parameters}$)	
	Model I, exponential vertices	Model II, power vertices
$P(s,t) = O(s,t) = 0$	1.779 (26)	1.636 (26)
$P(s,t)$, $O(s,t) \neq 0$	1.402 (31)	1.371 (32)

TABLE III. Parameters of Models I and II obtained by fitting to the data. Parameters α' and b are given in GeV^{-2}, z_0 is given in GeV^2, other parameters are dimensionless. Errors are taken from the MINUIT output.

	Model I exponential vertices		Model II power vertices	
Parameter	Value	Error	Value	Error
z_0	48.438	4.127	25.438	0.644
$g_1^{\mathcal{P}}$	0.314	0.006	0.358	0.002
$g_2^{\mathcal{P}}$	1.398	0.059	−0.007	0.001
$g_3^{\mathcal{P}}$	21.215	1.164	1.843	0.22
$g_1^{\mathcal{O}}$	−1.018	0.062	−0.174	0.004
$g_2^{\mathcal{O}}$	0.656	0.104	1.643	0.020
$g_3^{\mathcal{O}}$	−11302.3	6404.7	−491.034	3.079
r_+	0.281	0.003	0.372	0.001
r_-	0.682	0.009	0.201	0.001
$b_1^{\mathcal{P}}$	3.705	0.054	0.687	0.004
$b_2^{\mathcal{P}}$	1.387	0.015	4.580	0.265
$b_3^{\mathcal{P}}$	3.035	0.064	0.180	0.022
$b_1^{\mathcal{O}}$	2.471	0.044	1.163	0.008
$b_2^{\mathcal{O}}$	1.569	0.054	1.151	0.005
$b_3^{\mathcal{O}}$	151.69	28.98	0.419	0.001
$\alpha_+(0)$	0.670	0.011	0.585	0.004
$\alpha_-(0)$	0.467	0.012	0.461	0.007
α'_+	0.84	Fixed	0.84	Fixed
$\alpha'-$	0.93	Fixed	0.93	Fixed
g_+	74.218	2.506	74.889	1.164
g_-	58.270	3.682	60.033	2.247
b_+	0.0	Fixed	7.478	0.536
b_-	3.834	1.058	99.607	30.374
α'_P	0.414	0.010	0.368	0.002
α'_O	0.158	0.003	0.149	0.001
g_P	16.772	0.923	41.892	0.192
b_P	0.455	0.037	1.444	0.012
g_O	−0.063	0.005	226.083	1.753
b_O	0.0	Fixed	0.706	0.002
g_{r+}	−39.575	1.481	−6.578	0.078
g_{i+}	−10.945	0.477	0.132	0.072
$t_{\rm Ev}$	0.503	0.006	1.013	0.005
g_{r-}	76.320	5.872	−0.007	0.002
g_{i-}	0.4083	0.541	−0.058	0.004
$t_{\rm Od}$	0.083	0.010	4.205	0.116

$$\upsilon(t) = \begin{cases} \exp\left(2m_\pi - \sqrt{4m_\pi^2 - t}\right) & \text{for even terms,} \\ \exp\left(3m_\pi - \sqrt{9m_\pi^2 - t}\right) & \text{for odd terms.} \end{cases} \quad (25)$$

This first analysis gives a ground for three important inferences.

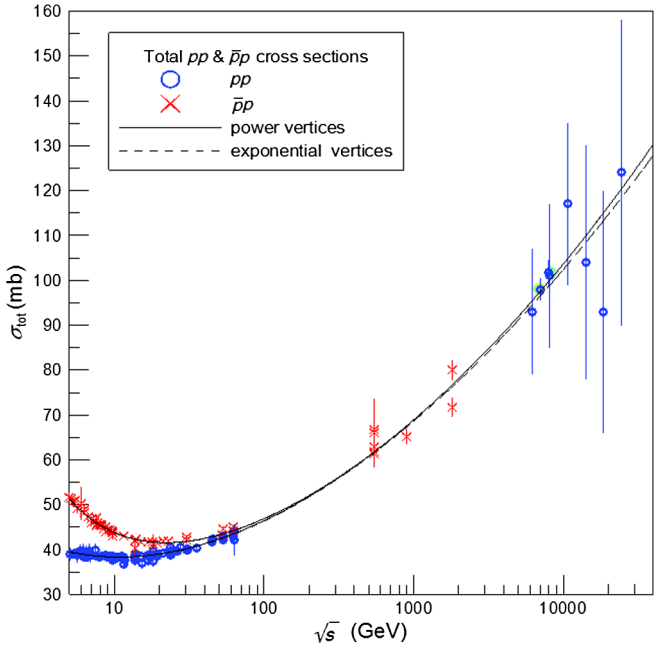

FIG. 1 (color online). pp and $\bar{p}p$ total cross sections.

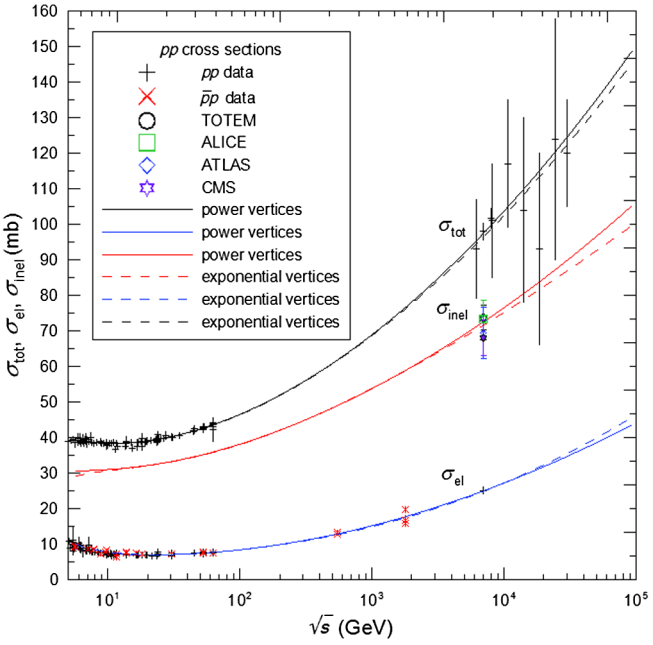

FIG. 3 (color online). Total, elastic, and inelastic pp cross sections.

(i) There are not any unusual or unexpected phenomena in new TOTEM data. They correspond to the standard Regge-like behavior at low and intermediate $|t|$.

(ii) The data at relatively low energies but at highest measured $|t|$ require in amplitude the terms decreasing like $1/(-t)^4$. It can be an indication of a hard scattering. However, taking into account that slow decreasing with t is obtained in the eikonal and U-matrix models [7], one can think that a powerlike behavior may be imitated by series of rescatterings or multi-Reggeon exchanges.

(iii) We believe that a successful description of the data in the considered models results from the well tuned structure of Pomeron and Odderon singularities [Eqs. (9) and (12)] rather than from a choice of vertex functions.

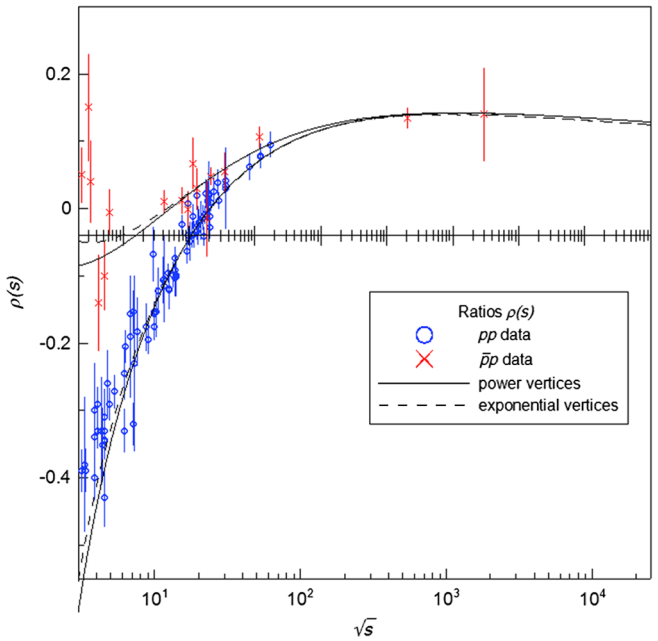

FIG. 2 (color online). Real to imaginary ratios of the forward scattering pp and $\bar{p}p$ amplitudes.

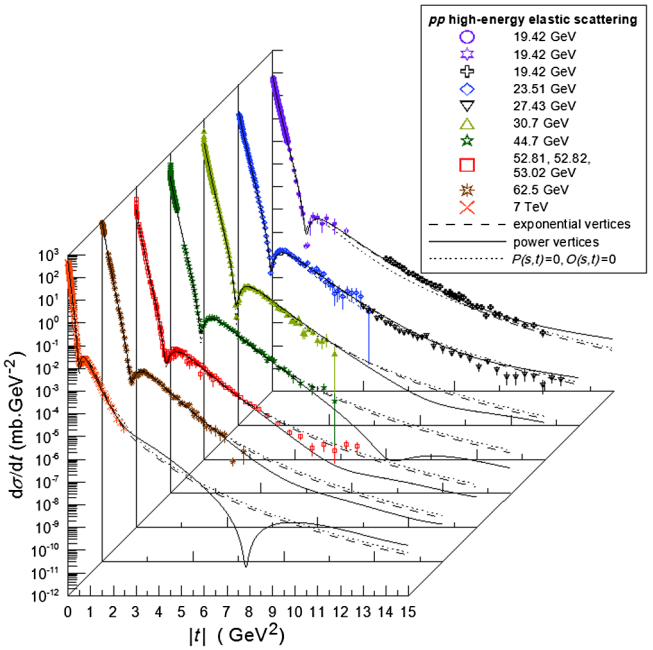

FIG. 4 (color online). Differential cross sections of pp elastic scattering.

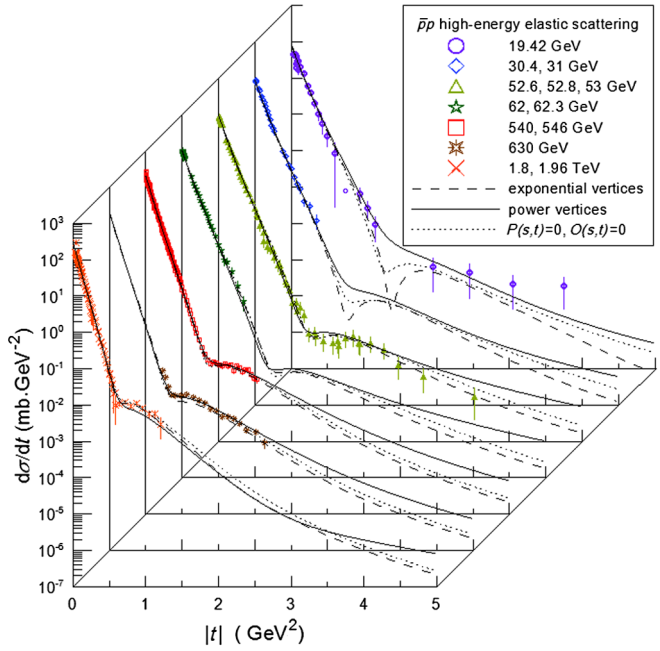

FIG. 5 (color online). Differential cross sections of $\bar{p}p$ elastic scattering.

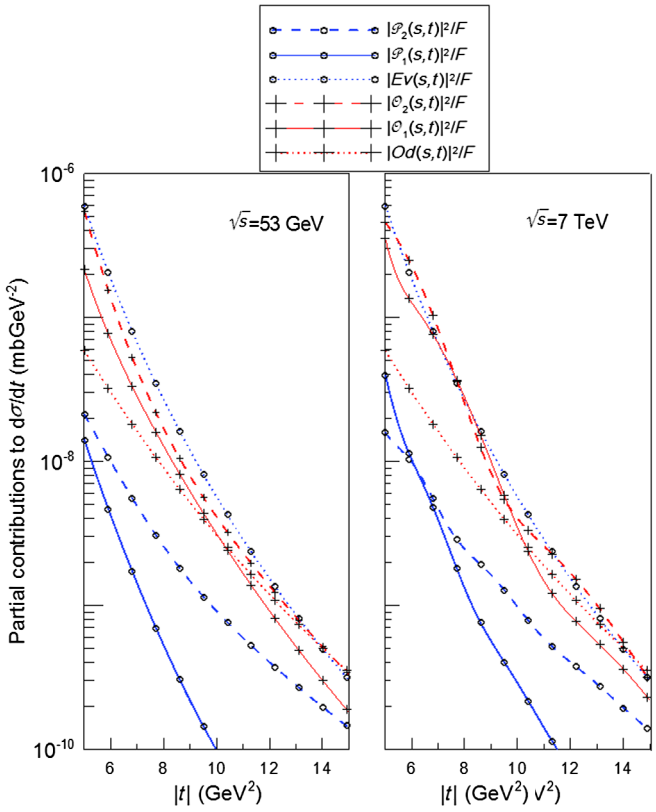

FIG. 6 (color online). Even and odd components of pp elastic scattering amplitudes at 53 GeV and 7 TeV (calculated in Model II). Factor F is defined in Eq. (23).

The theoretical curves for $\sigma_{\rm tot}(s)$, $\rho(s)$ and integrated elastic cross sections, $\sigma_{\rm el}(s)$, as well as for inelastic cross section, $\sigma_{\rm inel}(s)$, are shown in Figs. 1–3. The values of the total cross sections obtained at 7 and 8 TeV are a little bit less than the TOTEM data but they are within the measured errors. Both model predictions for higher LHC energies are given in Tables IV and V.

Description of the differential cross section in the models is demonstrated in Figs. 4 and 5. For the simplest model, i.e., at $P(s,t) = O(s,t) = 0$, we have shown curves only for a model with exponential vertices in order to avoid a meshing figure. From Table II, one can see that quality of description in both models is almost the same. The TOTEM $d\sigma/dt$ data are described with $\chi^2/N_p = 0.47$ and $\chi^{2/}N_p = 0.46$ in Models I and II [with $P(s,t)$, $O(s,t) \neq 0$], correspondingly.

We would like to stress that in spite of a widespread opinion that at high energy and high momentum transfers an Odderon contribution is dominating we found that in the considered models it is not the case. One can see in Figs. 6 and 7 that the dominating partial even and odd components at large $|t|$ have comparable values (at least for $|t| < 15$ GeV^2). However, Fig. 7 shows that cumulative even contribution to ds/dt at $|t|$ outside of the dip positions (see below) is larger of the odd one. The cumulative even contribution in this region at 7 TeV is a few times larger than the cumulative odd one. At the same time a role of odd contributions is important at low and intermediate t values and, especially, in the regions of dips.

In Fig. 8 we give the predictions of the considered models for the TOTEM experiment at higher transferred momenta and higher LHC energies. The most interesting point is an existing/absence of the second dip in $d\sigma/dt$. The model with exponential form factors leads

TABLE IV. Cross sections and ratio of real to imaginary parts of the forward scattering pp amplitude in Model I [with $P(s,t)$, $O(s,t) \neq 0$ and exponential vertices].

$\sqrt{s}$ (TeV)	$\sigma_{\rm tot}$ (mb)	$\sigma_{\rm el}$ (mb)	$\sigma_{\rm inel}$ (mb)	ρ
7	96.46	24.87	71.59	0.132
8	98.65	25.72	72.93	0.132
13	106.93	29.04	77.89	0.129
14	108.23	29.57	78.67	0.128

TABLE V. Cross sections and ratio of real to imaginary parts of the forward scattering pp amplitude in Model II [with $P(s,t)$, $O(s,t) \neq 0$ and power vertices].

$\sqrt{s}$ (TeV)	$\sigma_{\rm tot}$ (mb)	$\sigma_{\rm el}$ (mb)	$\sigma_{\rm inel}$ (mb)	ρ
7	97.48	24.97	72.51	0.136
8	99.76	25.77	73.98	0.135
13	108.37	28.85	79.52	0.132
14	109.73	29.33	80.39	0.132

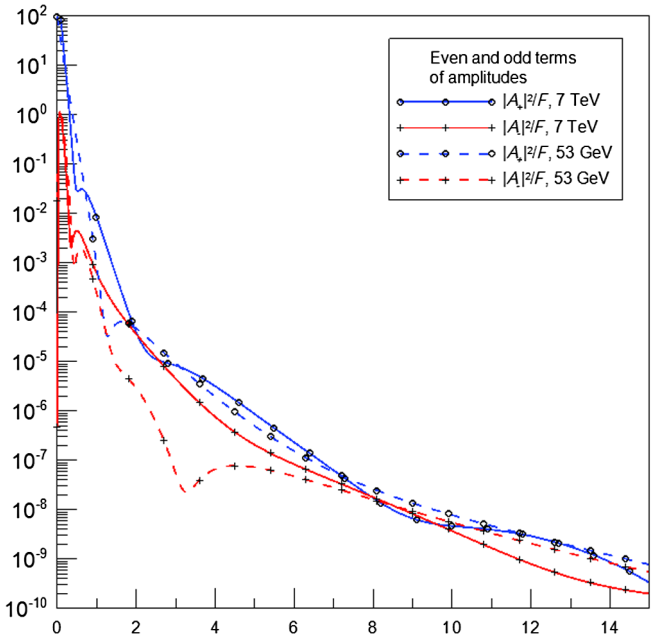

FIG. 7 (color online). Even and odd cumulative contributions to $d\sigma/dt$ at 53 GeV and 7 TeV (calculated in Model II). Factor F is defined in Eq. (23).

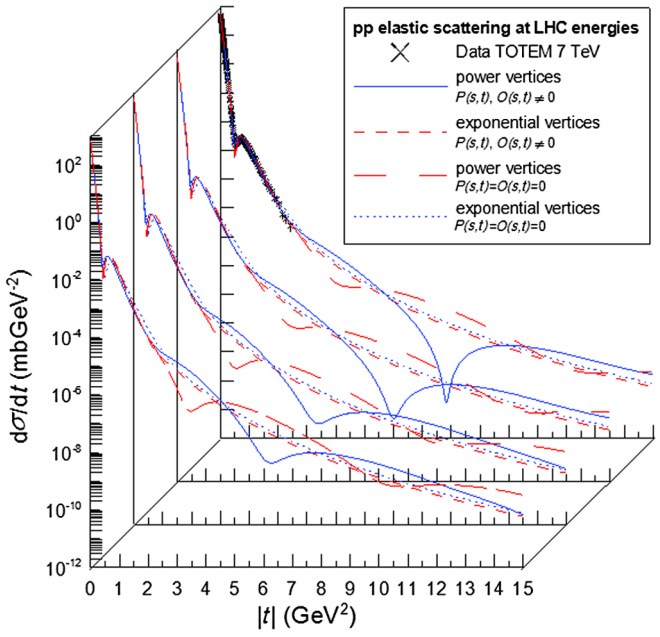

FIG. 8 (color online). Predictions of the models for pp differential cross sections at the LHC energies.

to smooth behavior with no dips, whereas, models with power vertices predict a dip structure in $d\sigma/dt$. If $P(s,t) = O(s,t) = 0$ then the shoulder at $|t| \approx 4$ GeV^2 and $\sqrt{s} = 7$ TeV is transformed into a dip moving to $|t| \approx 3$ GeV^2 at 14 TeV. Moreover, in this model the third dip is visible at the energy 14 TeV near $|t| \sim 10$ GeV^2. If $P(s,t), O(s,t) \neq 0$ then well pronounced dip develops at $|t| \approx 8$ GeV^2 moving to $|t| \approx 6$ GeV^2 when energy is increasing from 7 to 14 GeV. Accurate measurements at such $|t|$ would be the excellent test for the considered models.

IV. CONCLUSION

The analysis performed above demonstrated a high credibility of the tripole Pomeron-Odderon model developed in [4]. We have made its minor improvement only by adding two terms, crossing even $[E(s,t)]$ and odd $[\mathrm{Od}(s,t)]$, in order to apply the model to high t. We have considered two choices of t dependence in vertex functions and found in all the cases a good description of the data in a wide region of s and t even in the simplified versions of the model without the standard simple pole Pomeron and Odderon contributions. Thus, it allows us to conclude that the model is quite stable under variations of the preasymptotic components and the form of vertex functions. Apparently such the model stability is stipulated by the well tuned structure of the leading Pomeron $\mathcal{P}$ and Odderon $\mathcal{O}$ singularities.

The whole bulk of high energy data are described in a framework of the traditional Regge approach. In our opinion the new data in the TeV energy region do not show any indication of new unusual phenomena.

We have predicted the values of the total, elastic, and inelastic cross sections, as well as the ratio $\rho(s)$ and differential cross sections at higher LHC energies. The amazing prediction is made for the large $|t|$ region at the LHC energies. The model with an exponential t dependence of vertices leads to a smooth behavior of differential pp cross sections while in the model with power vertices a dip structure moving with energy is generated at large $|t|$. We hope that future measurements of the TOTEM collaboration will allow us to discriminate within possibilities for the developed model.

ACKNOWLEDGMENTS

I would like to thank my colleagues J. R. Cudell, V. Petrov, A. Prokudin, J. P. Revol, S. Troshin, and G. Zinovjev for numerous fruitful discussions of the Regge approaches and high-energy models, for reading the manuscript, and valuable remarks. The work is supported partially by the Physics and Astronomy Department of National Academy of Sciences of Ukraine (Agreement No. 2013).

[1] G. Antchev *et al.* (TOTEM Collaboration), Europhys. Lett. **95**, 41001 (2011).
[2] G. Antchev *et al.* (TOTEM Collaboration), Europhys. Lett. **101**, 21002 (2013).
[3] G. Antchev *et al.* (TOTEM Collaboration), Europhys. Lett. **101**, 21004 (2013).
[4] E. Martynov, Phys. Rev. D **76**, 074030 (2007).
[5] A. A. Godizov, AIP Conf. Proc. **1523**, 145 (2012).
[6] I. M. Dremin, Phys. Usp. **56**, 3 (2013).
[7] A. Alkin, O. Kovalenko, and E. Martynov, Europhys. Lett. **102**, 31001 (2013).
[8] V. A. Petrov and A. V. Prokudin, Eur. Phys. J. C **23**, 135 (2002).
[9] V. A. Petrov and A. V. Prokudin, Phys. Rev. D **87**, 036003 (2013).
[10] S. M. Troshin and N. E. Tyurin, Phys. Part. Nucl. **35**, 555 (2004); arXiv:hep-ph/0308027, and references therein.
[11] P. Gauron, E. Leader, and B. Nicolescu, Phys. Lett. B **238**, 406 (1990).
[12] R. Avila, P. Gauron, and B. Nicolescu, Eur. Phys. J. C **49**, 581 (2007).
[13] E. Martynov and B. Nicolescu, Eur. Phys. J. C **56**, 57 (2008).
[14] S. M. Troshin, Phys. Lett. B **682**, 40 (2009).
[15] J. R. Cudell, A. Lengyel, and E. Martynov, Phys. Rev. D **73**, 034008 (2006).
[16] J. Beringer *et al.*, Phys. Rev. D **86**, 010001 (2012); http://pdg.lbl.gov/2012/hadronic-xsections/.
[17] M. R. Whalley *et al.* (Durham Database Group), http://durpdg.dur.ac.uk/hepdata/.
[18] V. M. Abazov *et al.* (D0 Collaboration), Phys. Rev. D **86**, 012009 (2012).
[19] A file with the data "alldata-v2.zip" is available at http://www.theo.phys.ulg.ac.be/alldata-v2.zip.